Cell Reports, Volume *38*

Supplemental information

Lipid droplet dynamics regulate adult muscle stem cell fate

Feng Yue, Stephanie N. Oprescu, Jiamin Qiu, Lijie Gu, Lijia Zhang, Jingjuan Chen, Naagarajan Narayanan, Meng Deng, and Shihuan Kuang

Figure S1

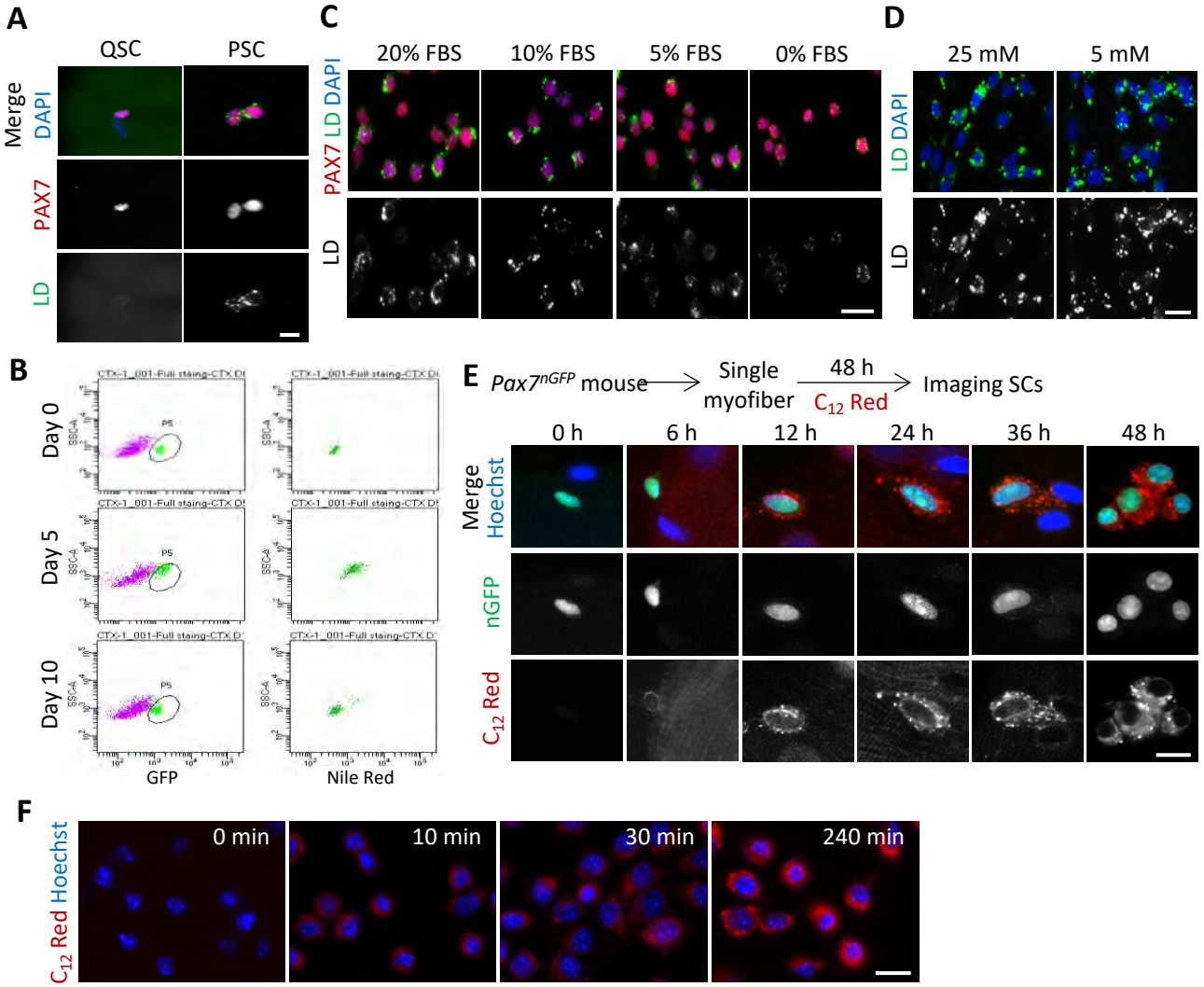
A
QSC
PSC
Merge
DAPI
PAX7
LD
C
20% FBS
10% FBS
5% FBS
0% FBS
PAX7 LD DAPI
LD
D
25 mM
5 mM
LD DAPI
LD
B
Day 0
Day 5
Day 10
GFP
Nile Red
E
Pax7nGFP mouse
Single myofiber
48 h
C12 Red
Imaging SCs
0 h
6 h
12 h
24 h
36 h
48 h
Merge Hoechst
nGFP
C12 Red
F
C12 Red Hoechst
0 min
10 min
30 min
240 min

Figure S1. Fatty Acid, But Not Glucose Contributes to LD Formation in SCs.

(A) Representative images of LDs (labeled in green with BODIPY493/503) in quiescent and proliferating SCs (QSCs and PSCs, $PAX7^{+}$) attached on host myofibers cultured for 0 h (QSC) and 42 h (PSC). Scale bar, 10 μm.

(B) Representative dot plot showing increased LD contents in activated SCs compared to quiescent SCs and self-renewed SCs during muscle regeneration.

(C) Immunostaining of SC-derived primary myoblasts cultured with gradient serum conditions for 24 h. LDs were identified by BODIPY493/503 (green), nuclei were counterstained with DAPI. Scale bar, 20 μm.

(D) LDs in SC-derived primary myoblasts cultured with 25 mM and 5 mM glucose for 24 h. Scale bar, 20 μm.

(E) Live cell fatty acid tracing with C_{12} Red (BODIPY558/568 C_{12}, a red fluorescent fatty acid) in cultured *Pax7*^{nGFP} myofibers. Nuclei were counterstained with Hoechst. Scale bar, 10 μm.

(F) Live cell fatty acid tracing with C_{12} Red in cultured SC-derived primary myoblasts. Scale bar, 20 μm.

Related to Figure 1.

Figure S2

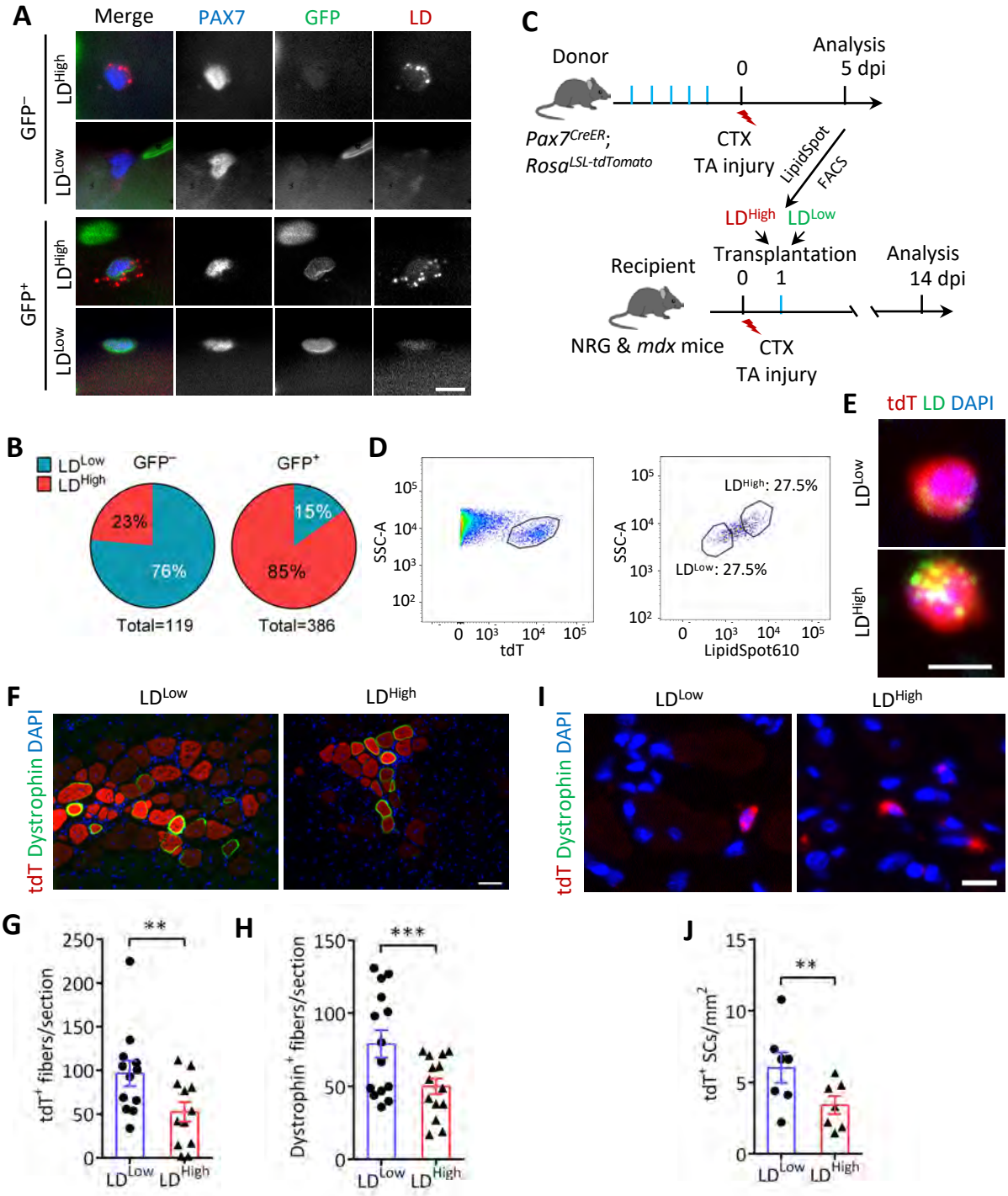
A
Merge
PAX7
GFP
LD
GFP⁻
LDHigh
LDLow
GFP⁺
LDHigh
LDLow
C
Donor
0
Analysis
5 dpi
Pax7CreER;
RosaLSL-tdTomato
CTX
TA injury
LipidSpot
FACS
LDHigh
LDLow
Transplantation
Recipient
0
1
Analysis
14 dpi
NRG & mdx mice
CTX
TA injury
B
LDLow
LDHigh
GFP⁻
GFP⁺
23%
76%
15%
85%
Total=119
Total=386
D
SSC-A
tdT
LDHigh: 27.5%
LDLow: 27.5%
LipidSpot610
E
tdT LD DAPI
LDLow
LDHigh
F
LDLow
LDHigh
tdT Dystrophin DAPI
I
LDLow
LDHigh
tdT Dystrophin DAPI
G
tdT⁺ fibers/section
**
LDLow
LDHigh
H
Dystrophin⁺ fibers/section
***
LDLow
LDHigh
J
tdT⁺ SCs/mm²
**
LDLow
LDHigh

Figure S2. LD^{Low} SCs display higher clonal and self-renewal capacity than LD^{High} SCs.

(A) Representative images of LDs in single SCs on *Myf5Cre*;*Rosa26*^{sfGFP} myofibers cultured for 48 h. GFP^{-} and GFP^{+} indicate stem and committed SCs, respectively. LDs were identified by LipidTOX (Red). Scale bar, 10 μm.

(B) Quantification of the LD^{Low} and LD^{High} cell percentage in GFP^{-} and GFP^{+} single SCs as shown in (A). n = 4 mice, total 119 GFP^{-} and 386 GFP^{+} SCs were analyzed.

(C) Experimental scheme showing the isolation of LD^{Low} and LD^{High} SCs and following transplantation design.

(D) Dot plot diagram of flow cytometry showing the population of LD^{Low} and LD^{High} SCs sorted for transplantation experiment.

(E) Representative images of LD^{Low} and LD^{High} SCs sorted for transplantation experiment. Scale bar, 10 μm.

(F and G) Representative images showing tdT^{+} myofibers (F) and quantification of the number of tdT^{+} myofibers (G) in regenerated muscles of *mdx* mice transplanted with FACS-isolated LD^{Low} and LD^{High} SCs at 14 dpi. n = 12 mice. Scale bar, 50 μm.

(H) Quantification of the number of dystrophin^{+} myofibers in regenerated muscles of *mdx* mice. n = 12 mice. Scale bar, 50 μm.

(I and J) Representative images showing tdT^{+} SCs (I) and quantification of the number of tdT^{+} SCs (J) in regenerated muscles of *mdx* mice transplanted with FACS-isolated LD^{Low} and LD^{High} SCs at 14 dpi. n = 7 mice. Scale bar, 10 μm.

Data are presented as mean ± SD; Student's t-test. $^{**}P < 0.01$, $^{***}P < 0.001$.

Related to Figure 2.

Figure S3

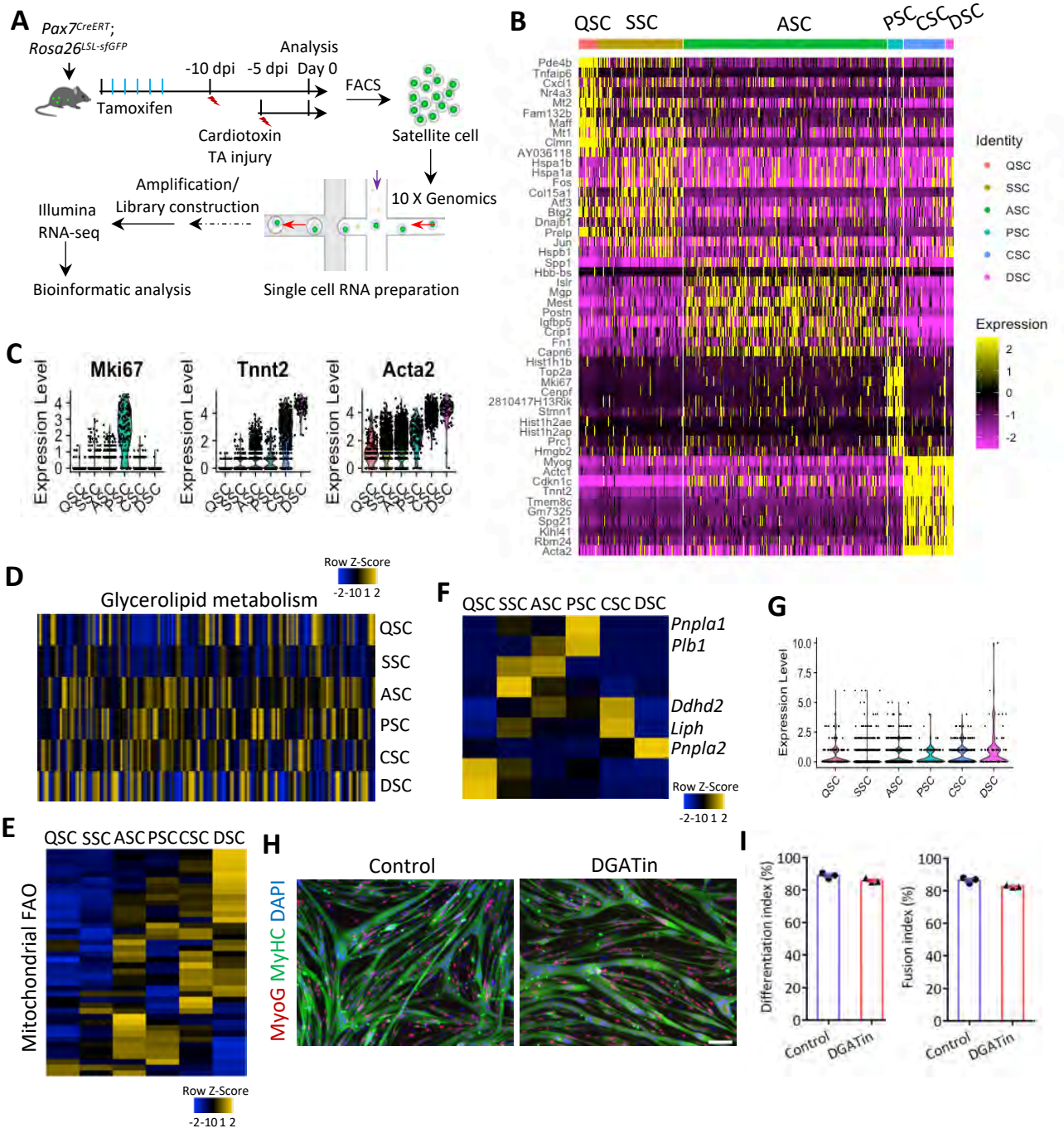
A
Pax7CreERT;
Rosa26LSL-sfGFP
Tamoxifen
-10 dpi
-5 dpi
Analysis
Day 0
FACS
Cardiotoxin
TA injury
Satellite cell
10 X Genomics
Amplification/
Library construction
Illumina
RNA-seq
Bioinformatic analysis
Single cell RNA preparation
B
QSC SSC ASC PSC CSC DSC
Identity
QSC
SSC
ASC
PSC
CSC
DSC
Expression
C
Mki67
Tnnt2
Acta2
Expression Level
D
Glycerolipid metabolism
Row Z-Score
-2-10 1 2
QSC
SSC
ASC
PSC
CSC
DSC
E
QSC SSC ASC PSC CSC DSC
Mitochondrial FAO
Row Z-Score
-2-10 1 2
F
QSC SSC ASC PSC CSC DSC
Pnpla1
Plb1
Ddhd2
Liph
Pnpla2
Row Z-Score
-2-10 1 2
G
Expression Level
QSC
SSC
ASC
PSC
CSC
DSC
H
Control
DGATin
MyoG MyHC DAPI
I
Differentiation index (%)
Fusion index (%)
Control
DGATin

Figure S3. Enrichment of Lipid Metabolic Genes in Committed and Differentiating SCs.

(A) Experimental scheme showing SC tagging and isolation from non-injured and cardiotoxin (CTX)–injured TA muscles at 5 dpi and 10 dpi for scRNA-seq analysis. n=3 mice for each condition.

(B) Heatmap visualizing the top 10 markers to determine specificity aiding with nomenclature for cluster identities.

(C) Violin plot showing the expression of SC markers at various stages informing cluster annotation of subpopulation.

(D) Heatmap of the annotated Gene Ontology term glycerolipid metabolic process genes in various SC cluster.

(E) Heatmap showing the enrichment of mitochondrial FAO pathway (GO:0006635) in in various SC cluster.

(F) Heatmap of the genes annotated in triglyceride catabolic process (GO:0019433) in various SC cluster.

(G) Violin plot showing the expression of *Pnpla2* at various SC stages.

(H and I) Representative immunostaining of MyoG and MyHC (H) and quantification of differentiation and fusion index (I) in cultures of differentiated myotubes treated with DGAT inhibitors for 2 days. $n = 3$. Scale bar, 50 μm.

Related to Figure 3.

Figure S4

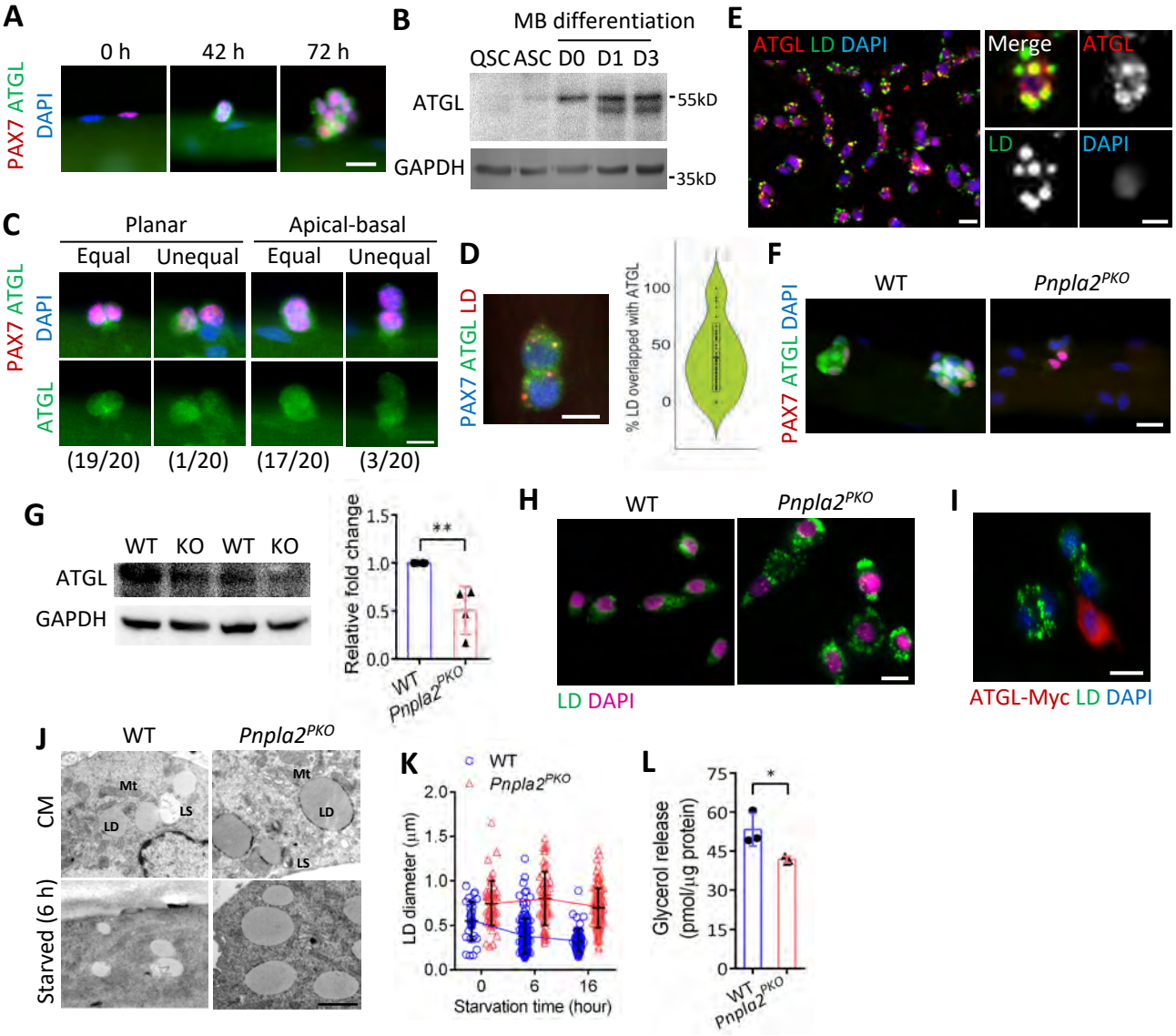
A
0 h
42 h
72 h
PAX7 ATGL DAPI
B
MB differentiation
QSC ASC D0 D1 D3
ATGL
55kD
GAPDH
35kD
E
ATGL LD DAPI
Merge
ATGL
LD
DAPI
C
Planar
Apical-basal
Equal
Unequal
Equal
Unequal
PAX7 ATGL DAPI
ATGL
(19/20)
(1/20)
(17/20)
(3/20)
D
PAX7 ATGL LD
% LD overlapped with ATGL
100
50
0
F
WT
Pnpla2PKO
PAX7 ATGL DAPI
G
WT KO WT KO
ATGL
GAPDH
Relative fold change
1.5
1.0
0.5
0.0
**
WT
Pnpla2PKO
H
WT
Pnpla2PKO
LD DAPI
I
ATGL-Myc LD DAPI
J
WT
Pnpla2PKO
CM
Starved (6 h)
Mt
LD
LS
K
WT
Pnpla2PKO
LD diameter (μm)
2.0
1.5
1.0
0.5
0.0
0
6
16
Starvation time (hour)
L
Glycerol release (pmol/μg protein)
75
60
45
30
15
0
*
WT
Pnpla2PKO

Figure S4. ATGL Targets to LDs for Lipolysis in Activated and Proliferating SCs.

(A) Immunostaining of ATGL in SCs on single myofibers cultured for 0 h, 42 h, and 72 h. Scale bar, 20 μm.

(B) Immunoblotting of ATGL in quiescent and activated SCs isolated by FACS from non-injured and injured (5dpi) muscles, and in cultured SC-derived primary myoblasts after induced for differentiation.

(C) Immunostaining of ATGL and quantification of the equal and unequal distribution of ATGL protein in SC doublets on single myofibers cultured for 48 h. Scale bar, 10 μm.

(D) Immunostaining images showing co-localization of LDs with ATGL in SCs on cultured single myofibers at 48 h, and violin plots showing percentage of LDs that co-localize with ATGL puncta. LDs were identified by LipidTOX (Red), nuclei were counterstained with DAPI (blue). n = 3 mice, 595 LDs in 76 SCs were analyzed. Scale bar, 10 μm.

(E) Immunostaining images showing co-localization of LD with ATGL in cultured SC-derived primary myoblasts. LDs were identified by BODIPY493/503. Scale bar, 20 μm.

(F) Immunostaining images showing depletion of ATGL in cultured SCs attached to a single myofiber isolated from *Pnpla2*^{PKO} mice (1 week after tamoxifen induced knockout), leading reduced cell number. Nuclei were counterstained with DAPI.

(G) Western blot analysis of WT and *Pnpla2*^{PKO} primary myoblasts confirming the depletion of ATGL.

(H) Immunostaining images showing increased LD accumulation in *Pnpla2*^{PKO} SC-derived primary myoblasts. LDs were identified by BODIPY493/503. Scale bar, 10 μm.

(I) Immunostaining ATGL and LDs in primary myoblasts 36 h after transfection of pKMyc-ATGL plasmid. Scale bar, 10 μm.

(J and K) TEM images (J) and LD diameter distribution (K) in WT and *Pnpla2*^{PKO} SC-derived primary myoblasts cultured under serum starvation conditions. Number of LD quantified at 0 h, WT: n = 32, *Pnpla2*^{PKO}: n = 56; at 6 h, WT: n = 141, *Pnpla2*^{PKO}: n = 66; at 16 h, WT: n = 63, *Pnpla2*^{PKO}: n = 106. LD: lipid droplet, LS: lysosome, Mt: mitochondria. Scale bar, 1 μm.

(L) Glycerol release, as an indicator of lipolysis, measured as glycerol content in culture medium normalized to total protein level of cultured FACS-sorted WT and *Pnpla2*^{PKO} SCs. n = 3 mice.

Data are presented as mean ± SD; Student's t-test. *$P < 0.05$, **$P < 0.01$.

Related to Figure 4.

Figure S5

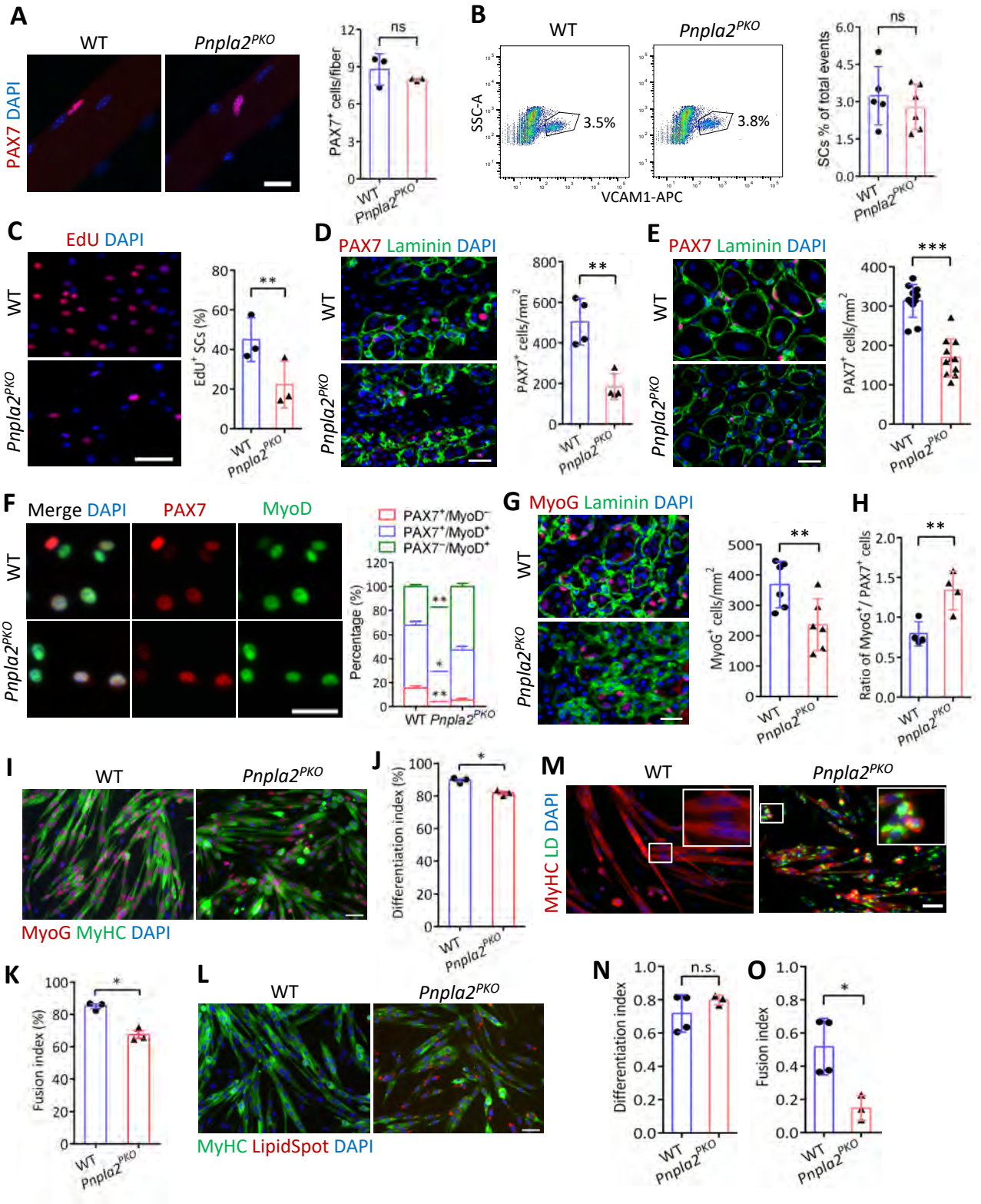
A
WT
Pnpla2PKO
PAX7 DAPI
PAX7+ cells/fiber
ns
B
WT
Pnpla2PKO
SSC-A
3.5%
3.8%
VCAM1-APC
SCs % of total events
ns
C
EdU DAPI
WT
Pnpla2PKO
EdU+ SCs (%)
**
D
PAX7 Laminin DAPI
PAX7+ cells/mm2
**
E
PAX7 Laminin DAPI
PAX7+ cells/mm2
***
F
Merge DAPI
PAX7
MyoD
PAX7+/MyoD−
PAX7+/MyoD+
PAX7−/MyoD+
Percentage (%)
G
MyoG Laminin DAPI
MyoG+ cells/mm2
**
H
Ratio of MyoG+ / PAX7+ cells
**
I
WT
Pnpla2PKO
MyoG MyHC DAPI
J
Differentiation index (%)
*
M
WT
Pnpla2PKO
MyHC LD DAPI
K
Fusion index (%)
*
L
WT
Pnpla2PKO
MyHC LipidSpot DAPI
N
Differentiation index
n.s.
O
Fusion index
*

Figure S5. ATGL Is Required for Myogenic Function of SCs.

(A) Immunostaining and quantification of QSC number on WT and *Pnpla2*^{PKO} myofibers 1 week after TMX treatment *in vivo.* $n = 3$ mice. Scale bar, 20 μm.

(B) Dot plot diagram of flow cytometry and quantification of QSC number in WT and *Pnpla2*^{PKO} muscles 1 week after TMX treatment *in vivo.* WT: $n = 5$ mice, *Pnpla2*^{PKO}: $n = 6$ mice. QSC number was showed by percentage of total events.

(C) EdU labeling and quantification in FACS-isolated SCs after 12 h of pulsing. $n = 3$ mice, average 654 cells were analyzed from each mice. Scale bar, 50 μm.

(D and E) Immunostaining of PAX7 and quantification of PAX7^{+} SC number on cross-sections of young adult WT and *Pnpla2*^{PKO} TA muscles at 3.5 (D) and 5.5 dpi (E). 3.5 dpi: $n = 4$ mice, 5.5 dpi: $n = 11$ mice. Scale bar, 50 μm.

(F) Representative PAX7 and MyoD immunostaining and quantification in cultured FACS-sorted SCs showing the reduction of self-renewing (PAX7^{+}/MyoD$^{–}$) SCs and increase of committed (PAX7$^{–}$/MyoD^{+}) SCs. WT: $n = 5$ mice, *Pnpla2*^{PKO}: $n = 4$ mice, 3666 SCs in WT and 635 SCs in *Pnpla2*^{PKO} mice were analyzed. Scale bar, 50 μm.

(G) Immunostaining of MyoG and quantification of MyoG^{+} cell number on cross-sections of young adult WT and *Pnpla2*^{PKO} TA muscles at 3.5 dpi. $n = 6$ mice. Scale bar, 50 μm.

(H) Ratio of MyoG^{+} to PAX7^{+} cells on muscle cross-sections at 3.5 dpi showing in (F) and (J). $n = 4$ mice.

(I-K) Immunostaining of MyoG and MyHC in differentiated myotubes (I), and quantification of differentiation (J) and fusion index (K). FACS-isolated SCs from WT and *Pnpla2*^{PKO} resting muscles were plated and immediately differentiated upon attachment for 2 days. $n = 3$ mice. Scale bar, 20 μm.

(L) Immunostaining of MyHC and LDs in differentiated myotubes. Scale bar, 20 μm.

(M-O) Immunostaining of MyHC and LDs in differentiated myotubes (M), and quantification of differentiation (N) and fusion index (O). FACS-isolated SCs from WT and *Pnpla2*^{PKO} resting muscles were cultured for 7 days and induced differentiation for 2 days. WT: $n = 4$ mice; *Pnpla2*^{PKO}: $n = 3$ mice. Scale bar, 50 μm.

Data are presented as mean ± SD; Student's *t*-test. *$P < 0.05$, **$P < 0.01$, ***$P < 0.001$, n.s., no significance.

Related to Figure 4.

Figure S6

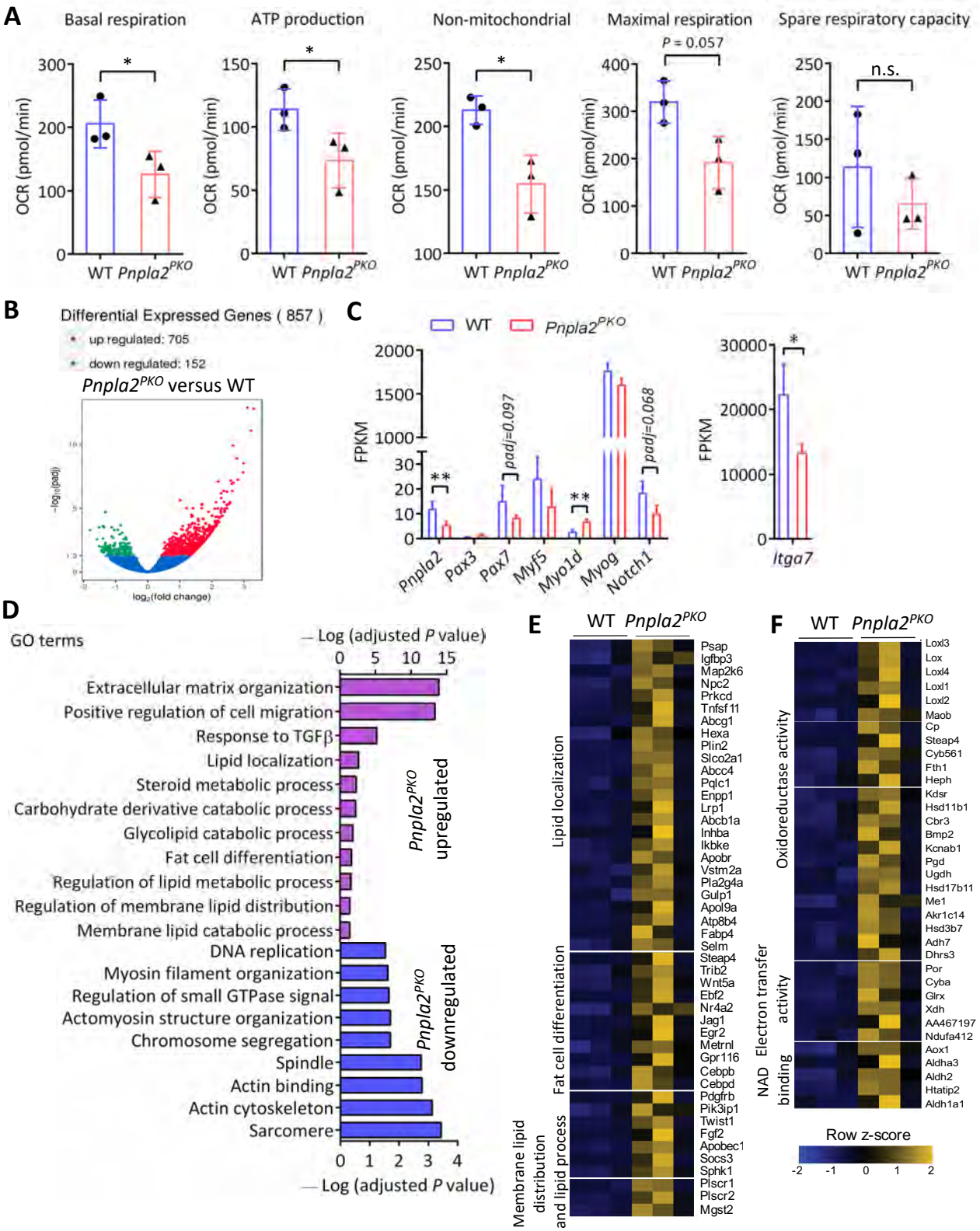
A
Basal respiration
ATP production
Non-mitochondrial
Maximal respiration
Spare respiratory capacity
OCR (pmol/min)
P = 0.057
n.s.
WT
Pnpla2PKO
B
Differential Expressed Genes (857)
up regulated: 705
down regulated: 152
Pnpla2PKO versus WT
C
WT
Pnpla2PKO
FPKM
padj=0.097
padj=0.068
Pnpla2
Pax3
Pax7
Myf5
Myo1d
Myog
Notch1
Itga7
D
GO terms
Log (adjusted P value)
Extracellular matrix organization
Positive regulation of cell migration
Response to TGFβ
Lipid localization
Steroid metabolic process
Carbohydrate derivative catabolic process
Glycolipid catabolic process
Fat cell differentiation
Regulation of lipid metabolic process
Regulation of membrane lipid distribution
Membrane lipid catabolic process
DNA replication
Myosin filament organization
Regulation of small GTPase signal
Actomyosin structure organization
Chromosome segregation
Spindle
Actin binding
Actin cytoskeleton
Sarcomere
Pnpla2PKO upregulated
Pnpla2PKO downregulated
E
Lipid localization
Fat cell differentiation
Membrane lipid distribution and lipid process
F
Oxidoreductase activity
Electron transfer activity
NAD binding
Row z-score

Figure S6. Reduced Oxygen Consumption Rate and Global Changes of Genes Related to Energy Metabolism in *Pnpla2*^{PKO} SCs.

(A) OCR of cultured WT and *Pnpla2*^{PKO} SC-derived primary myoblasts with or without Etomoxir (50 μM for 15 min before the test). $n = 3$ independent experiments.

(B) Volcano diagram of differentially expressed genes in *Pnpla2*^{PKO} SCs versus WT control. Blue dots indicate genes without significant difference, red and dots indicate genes upregulated and downregulated in *Pnpla2*^{PKO} SCs. $n = 3$ mice.

(C) Expression of myogenic genes, *Notch1 and integrin α 7* (*ITGA7*) in WT and *Pnpla2*^{PKO} SCs derived from RNA-seq data.

(D) GO analysis shows biological processes enriched in *Pnpla2*^{PKO} SCs.

(E) Heatmap representing differential gene expression shows a global increase of lipid metabolism in *Pnpla2*^{PKO} SCs. $n = 3$ mice.

(F) Heatmap representing the upregulated genes related to oxidoreductase and electron transfer activity in *Pnpla2*^{PKO} SCs. $n = 3$ mice.

Data are presented as mean ± SD; Student's *t*-test. $*P < 0.05$, $**P < 0.01$, ns, no significance.

Related to Figure 6.

Figure S7

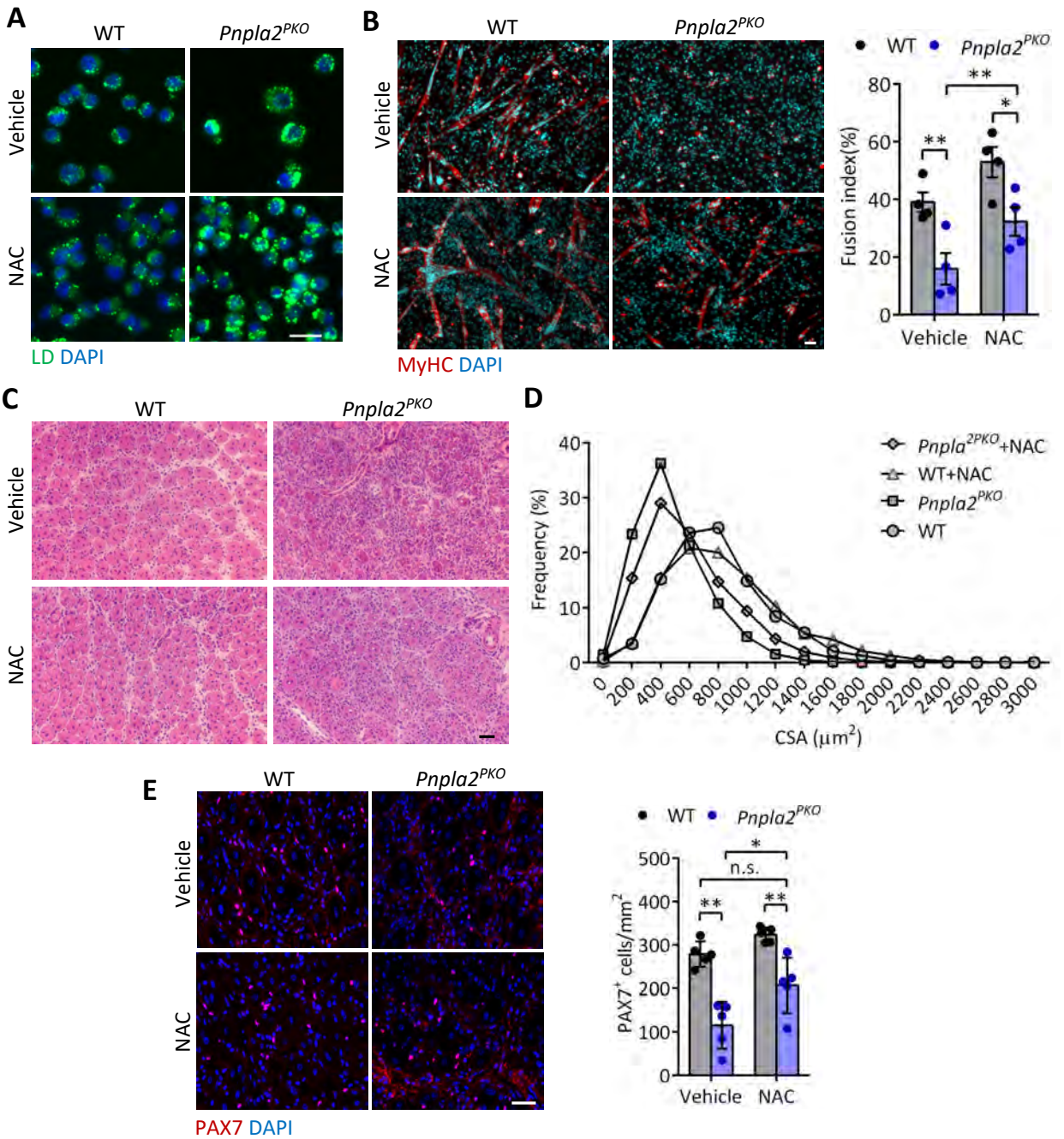
A
WT
Pnpla2PKO
Vehicle
NAC
LD DAPI
B
WT
Pnpla2PKO
Vehicle
NAC
MyHC DAPI
WT
Pnpla2PKO
Fusion index(%)
Vehicle
NAC
C
WT
Pnpla2PKO
Vehicle
NAC
D
Pnpla2PKO+NAC
WT+NAC
Pnpla2PKO
WT
Frequency (%)
CSA (μm2)
E
WT
Pnpla2PKO
Vehicle
NAC
PAX7 DAPI
WT
Pnpla2PKO
PAX7+ cells/mm2
n.s.
Vehicle
NAC

Figure S7. NAC Supplementation Partially Restores the Differentiation Potential of ATGL-deficient SCs and Muscle Regeneration.

(A) Representative images showing LDs in cultured FACS-sorted SCs with or without NAC (5 mM). Scale bar, 20 μm.

(B) Immunostaining of MyHC and quantification of fusion index in muscle cell mixture after 2 days differentiation cultured with or without NAC (5 mM). n = 4 mice in each condition. Scale bar, 50 μm.

(C) Hematoxylin and eosin (H&E) staining of TA muscle cross-sections from WT and *Pnpla2*^{PKO} mice with or without NAC treatment at 5.5 dpi. n = 4 mice in each condition. Scale bar, 50 μm.

(D) CSA distribution of dystrophin^{+} myofibers in TA muscle cross-sections from WT and *Pnpla2*^{PKO} mice with or without NAC treatment at 5.5 dpi. n = 5 mice. 2625, 1724, 2517, and 2171 myofibers were analyzed for WT, *Pnpla2*^{PKO}, WT+NAC and *Pnpla2*^{PKO}+NAC, respectively.

(E) Immunostaining of PAX7 and quantification of PAX7^{+} cell number on TA muscle cross-sections of WT and *Pnpla2*^{PKO} mice after NAC treatment at 5.5 dpi. Scale bar, 50 μm.

Data are presented as mean ± SD; Student's t-test. *P < 0.05, **P < 0.01, n.s. no significance.

Related to Figure 7.

Table S2. List of antibodies used in this study, Related to STAR Methods.

Antibody	Manufacture	Catalog #	Application
Mouse monoclonal anti-PAX7	DSHB	#PAX7	IF (1:10)
Mouse monoclonal anti-MyoD	Santa Cruz Biotechnology	sc-377460	IF (1:1000)
Mouse monoclonal anti-MyoG	DSHB	F5D	IF (1:1000)
Mouse monoclonal anti-MyHC	DSHB	MF-20	IF (1:100)
Mouse monoclonal anti-eMyHC	DSHB	F1.652	IF (1:100)
Rabbit polyclonal anti-Laminin	Sigma	L9393	IF (1:1000)
Rabbit polyclonal anti-Dystrophin	Abcam	ab15277	IF (1:1000)
Rabbit polyclonal anti-Ki67	Abcam	ab15580	IF (1:1000)
Rabbit polyclonal anti-ATGL	Cell Signaling	#2439	IF (1:200), IB (1:1000)
Mouse monoclonal anti-GAPDH	Santa Cruz Biotechnology	sc-32233	IB (1:3000)
PE Rat anti-mouse CD31 antibody	BD Biosciences	#553373	FACS (1:1000)
PE anti-mouse CD45 antibody	eBioscience	#12-0451-82	FACS (1:1000)
Pacific Blue anti-mouse Ly-6A/E (Sca-1) antibody	BioLegend	#122520	FACS (1:1000)
APC anti-mouse CD106 antibody	BioLegend	#105718	FACS (1:5000)
Alexa 568 goat anti-mouse IgG1	Invitrogen	A-21124	IF (1:1000)
Alexa 488 goat anti-mouse IgG1	Invitrogen	A-21121	IF (1:1000)
Alexa 647 goat anti-mouse IgG2b	Invitrogen	A-21242	IF (1:1000)
Alexa 488 goat anti-rabbit IgG	Invitrogen	A-11034	IF (1:1000)
Alexa 647 goat anti-rabbit IgG	Invitrogen	A-21244	IF (1:1000)
HRP AffiniPure goat anti-mouse IgG	Jackson ImmunoResearch	115-035-003	IB (1:10,000)
HRP AffiniPure goat anti-rabbit IgG	Jackson ImmunoResearch	111-035-003	IB (1:10,000)

Table S3. qPCR primer sequences, Related to STAR Methods.

Gene name	**Sequence (5' to 3')**
Pax7: forward	TCTCCAAGATTCTGTGCCGAT
Pax7: reverse	CGGGGTTCTCTCTCTTATACTCC
Myf5: forward	AAGGCTCCTGTATCCCCTCAC
Myf5: reverse	TGACCTTCTTCAGGCGTCTAC
Myogenin: forward	TGCCCAGTGAATGCAACTCC
Myogenin: reverse	TTGGGCATGGTTTCGTCTGG
Spry1: forward	GGTCATAGGTCAGATCGGGTC
Spry1: reverse	CTTGCCACACTGTTCGCAG
Plin2: forward	GACCTTGTGTCCTCCGCTTAT
Plin2: reverse	CAACCGCAATTTGTGGCTC
Gapdh: forward	AGGTCGGTGTGAACGGATTTG
Gapdh: reverse	TGTAGACCATGTAGTTGAGGTCA